JOURNAL OF OPTOELECTRONICS AND ADVANCED MATERIALS Vol. 13, No. 10, October 2011, p. 1331 - 1337

Al doped ZnO thick films as CO_2 gas sensors

ARUN PATIL*, CHANDRAKANT DIGHAVKAR, RATAN BORSE[a]
L.V.H. College, Panchavati, Nashik 422003, Maharashtra, India.
[a]Thin and Thick film Laboratory, Dept. of Electronics, M.S.G.College, Malegaon Camp 423105, Dist. Nashik, Maharashtra, India

Thick films of pure and Al doped ZnO with various concentrations (1 wt. %, 3 wt. %, 5 wt. %, 7 wt. % and 10 wt. %) of Al were prepared on alumina substrates using a screen printing technique. These films were fired at a temperature of 700ºC for two hours in an air atmosphere. Morphological, compositional and structural properties of the samples were studied using the scanning electron microscopy (SEM), Energy dispersive spectroscopy (EDAX) and X-ray diffraction techniques respectively. The gas sensing studies were carried out in a static gas sensing system under normal laboratory conditions. The surface resistance of thick films changes when exposed to CO_2 gas. The Al doped films show significant sensitivity to CO_2 gas than pure ZnO film. 10 wt. % Al-doped ZnO films were found to be more sensitive to CO_2 gas exposed at 250°C than other doping concentrations with fast response and comparatively slow recovery time.

(Received August 17, 2011; accepted October 20, 2011)

Keywords: ZnO, Al, Thick films, Screen printing, CO_2

1. Introduction

Nowadays, there is a great interest in implementing sensing devices in order to improve environmental and safety control of gases. There is also great needing of this kind of sensors to carry out the optimization of combustion reactions in the emerging transport industry and in domestic & industrial applications. Solid state gas sensors show fast sensing response, simple implementation and low prices [1, 2, 3]. Transition metal oxides such as TiO_2, SnO_2, WO_3, ZnO, In_2O_3 etc. appear to be best candidates for semiconductor gas sensors [1, 2, 4-9]. The sensitivity of these devices is based on the dependence of conductivity of metal oxides on the surrounding atmosphere. Nevertheless, full development of such devices require an improvement of their characteristics by the introduction of metal additives [10].These additives enhance the material sensitivity & selectivity & decrease the response time & the operating temperature of the sensing layer [11,12]. Another important property is that the presence of metallic additives can also modify the growth kinetic. The amount and distribution of the metal is the most important parameter to be controlled in order to obtain the highest sensitivity [13].

ZnO is an n-type semiconducting oxide of the group II metal zinc, and belongs to the P63mc space group [14]. The undoped ZnO has high n-type conductivity due to defects such as oxygen vacancies and Zn interstitials, which form donor levels [15]. ZnO has high transparency in the visible and near-ultraviolet spectral regions, wide conductivity range and conductivity changes under photoreduction/oxidation condition [16]. Accordingly this binary compound has wide applications in chemical sensors, heterojunction solar cells, electrophotography, surface acoustic wave devices, conductive transparent conductors and many others. However, pure ZnO films lack stability in terms of thermal edging in air or corrosive environments [17]. Therefore polycrystalline ZnO films doped metal ions such as indium (In), aluminum (Al), gallium (Ga), copper (Cu), cadmium (Cd) etc. have been reported to enhance their structural, optical and electrical properties [18]. Doping is particularly done to get high transparency, stability and high conductivity. Aluminium doping is particularly suitable for this purpose. Aluminium doped ZnO (AZO) films have high transmittance in the visible region, and a low resistivity, and the optical band gap can be controlled by using Al doping amount [19]. Accordingly they have got potential applications in solar cells, antistatic coatings, solid-state display devices, optical coatings, heaters, defrosters, chemical sensors etc. [19-21]. Al has been used to improve the electrical conductivity and thermal stability of ZnO films. For this work, Al^{3+} substitution on Zn^{2+} was chosen due to the small ion size of Al^{3+} compared to that of Zn^{2+} (r_{Al}^{3+} = 0.054 nm and r_{Zn}^{2+}=0.074 nm) [22].

Al doped films showed the potential to increase the gas response of ZnO films, since their performance is directly related to the exposed surface area, electrical and sensitivity characteristics [23-25].

Due to environmental concerns, carbon dioxide in the atmosphere needs to be monitored and controlled regularly. The atmosphere contains 0.038% CO_2 while the concentration of CO_2 in exhaled air was approximately 6%. The regulations from OSHA (Occupational Safety and Health Administration) limited CO_2 in the workplace to 0.5% for a prolonged period, and the U.S. National Institute for Occupational Safety and Health limited brief exposures (up to ten minutes) of CO_2 to 3% [26]. Recently, carbon dioxide (CO_2) gas sensor have attracted considerably attention for applications in greenhouse gases (GHGs) monitoring. This type of sensors is also required

for quality assurance of carbon dioxide used in soft drinks, mineral waters and beers according to The International Society of Beverage Technologists (ISBT) [27]. To assess the potential for such applications we investigated screen printed ZnO: Al films as sensing material for a novel carbon dioxide sensor.

2. Experimental

2.1 Materials

AR grade ZnO was used as a functional material. AR grade Al powder was used as a dopant. Glass frit (70 wt. % PbO, 18 wt. % Al_2O_3, 9wt. % SiO_2 and 3wt. % B_2O_3) was used as a permanent binder and ethyl cellulose (EC) was as local binder. Butyl carbitol acetate (BCA) was the vehicle used to prepare the paste of ZnO: Al material.

2.2 Screen printing process

The ZnO: Al pastes used in screen printing were prepared by maintaining the inorganic to organic materials ratio of 70:30. Inorganic part consists of a functional material (ZnO), dopant (Al) and glass frit. Organic parts consist of 8% ethyl cellulose (EC) and 92% butyl carbitol acetate (BCA). The Analar (AR) grade ZnO with x wt. % Al (x = 1, 3, 5, 7 and 10%) and 5 wt. % of glass frit were mixed thoroughly in an acetone medium with mortar and pestle. A solution of EC and BCA in the ratio 8:92 was made, which was added drop by drop to achieve the thixotropic properties of the paste. ZnO thick films were prepared on alumina substrates using a standard screen-printing technique. A nylon screen (40s, mesh no.355) was used for screen-printing. The required mask (2 x 1.25 cm) was developed on the screen using a standard photolithography process. The paste was printed on clean alumina substrates (5 x 2 cm) with the help of a mask. The pattern was allowed to settle for 15 to 20 minutes in air. The films were dried under infrared radiation for 45 minutes to remove the organic vehicle and then fired at a temperature of 700^oC for 2 h (which includes the time required to achieve the peak firing temperature , constant firing for 30 minutes at the peak temperature and then to attain the room temperature) in a muffle furnace. During the firing process glass frit melted and the functional material and dopant were sintered. The function of glass frit is to bind the grains of functional and dopant materials together and also to adhere the film firmly to the substrate surface.

2.3 Characterization

The structural properties of ZnO: Al films were investigated using X-ray diffraction analysis from 20-80^0 [Rigaku diffractometer (Miniflex Model, Rigaku, Japan) with CuKα, λ=0.1542 *nm* radiation] with a 0.1^o/step (2θ) at the rate of 2 s/step. A scanning electron microscopy (SEM- JOEL JED-2300) was employed to characterize the surface morphology. The composition of ZnO: Al thick film samples were analyzed by an energy dispersive X-ray spectrometer (JOEL-JED 6360 LA). The thickness of the films was measured using a Taylor-Hobson (Taly-step UK) system and was observed to be uniform in the range of 20μm to 25μm.

The average crystallite size was calculated from XRD pattern using following Debye Scherer's formula [28],

$$D = \frac{0.9\lambda}{\beta \cos\theta} \quad (1)$$

where, β = Full angular width of diffraction peak at the at half maxima peak intensity. λ = wavelength of X-radiation.

The average particle size was measured from SEM and specific surface area was calculated for spherical particles using the following equation [29].

$$S_W = \frac{6}{\rho d} \quad (2)$$

where d is the diameter of the particles, ρ is the composite density of the particles.

The D.C. resistance of the films was measured by using half bridge method in an air atmosphere at different temperatures. The gas sensing studies were carried out on a static gas sensing system under normal laboratory conditions. The electrical resistance of thick films in air (R_a) and in the presence of CO_2 vapour (R_g) was measured to evaluate the gas response (S) given by the relation,

$$Sensitivity(S) = \left| \frac{R_a - R_g}{R_a} \right| \times 100 \quad (3)$$

where R_a is the resistance of the ZnO: Al thick films in air and R_g is the resistance of the ZnO: Al thick films in CO_2 atmosphere.

The selectivity of the films for the particular gas with respect to other was determined by the relation,

$$\%\ Selectivity = \left(\frac{S_{other\ gas}}{S_{target\ gas}} \right) \times 100\% \quad (4)$$

Where S is sensitivity of the films

3. Result and discussion

3.1 Elemental Analysis

The elemental compositions of ZnO: Al films were analyzed using an energy dispersive spectrometer and is shown in Table.1. The mass% of Zn and O in each sample was not as per stoichiometric proportion. The ZnO film doped with 10 wt. % Al was observed to be most oxygen difficient. The deficiency of the constituent material

particles or an excess of it leads to the semiconducting behaviour of the material. [30]

Table 1. Composition of Al doped ZnO films.

Element (mass %)	Al				
	1wt. %	3wt. %	5wt. %	7wt. %	10wt. %
O	21.38	22.14	21.12	20.66	20.43
Zn	77.97	75.15	74.17	73.42	72.44
Al	0.65	2.71	4.71	5.92	7.13

3.2 Structural analysis

The crystalline structure of the films was analyzed with X-ray diffractogram in the 20-80^0 (2θ) range using Cuk$_\alpha$ radiation. **Figure 1** shows the XRD pattern of undoped and Al doped ZnO thick films of different concentrations. From the XRD pattern of Al doped ZnO films of different doping concentrations, the observed diffraction peaks correspond to the hexagonal wurtzite structure of ZnO (JCPDS 36- 1451). It has been observed that ZnO phase has preferred orientation in (101) plane. XRD pattern of all the films seem to be qualitatively similar. No metallic Al characteristic peak was observed. From 5 wt. % to 10 wt. % al doping, the slight increases in the intensity of strong orientation of alumina substrate (Al_2O_3) was observed. This may be due to Al replacing zinc substitutionally in the lattice or Al segregation to the non-crystalline regions in the grain boundary [31]. From 5wt. % to 10 wt. %, the excess Al was suppose to be converted into Al_2O_3. The average crystallite size was calculated from XRD pattern using Debye Scherer's formula represented by equation 1. The crystallite size of 10 wt. % Al doped films was observed as 17.47nm which is less than its value for other doping concentrations.

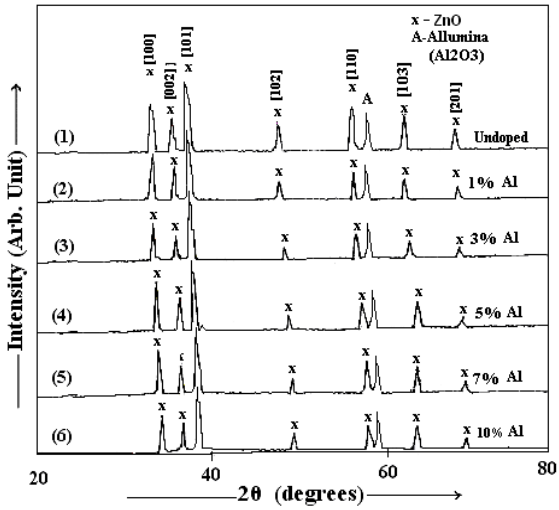

Fig.1 XRD pattern of pure ZnO and ZnO: Al films

3.3 Surface morphology analysis

It is well known that the gas sensing properties of a metal oxide thick film strongly depends on its morphological features. A high surface area facilitates the chemisorptions process by increasing the adsorption and desorption rates [32]. **Figure 2** indicates the SEM images of pure and x wt. % of Al (x = 1, 3, 5, 7 and 10 wt. %) thick films. **Fig. 2-(a)** shows the microstructure of pure ZnO thick film. It showed that the microstructure is nearly uniform with negligible open porosity. From **Fig.2-(b, c, d, e, f),** Formation of submicrometer crystallites distributed more or less uniformly over the surface. No cracks are detected. Some holes indicating porosity is present. Agglomeration of small crystallites also seems to be present in the certain region. The contrast difference is due to different orientations of the crystallites. The microstructure observation indicated that the Al addition decreased the grain growth at higher doping concentration. The particle size of pure ZnO films is more than Al doped ZnO films. As Al concentration increased upto 3 wt. %, the particle size increases and the surface roughness increases. For the further doping concentration of Al upto 10 wt. %, the particle size decreases and the surface roughness decreases. It may be due to segregation of Al to the non crystalline region in the boundary [33].

The specific surface area was calculated by using equation 2.The films doped with 10 wt. % Al showed higher specific surface area. The specific surface area increases as the size of the grains decreases [29]. **Table-2** presents the particle size and surface area of ZnO thick films doped with different wt. % of Al.

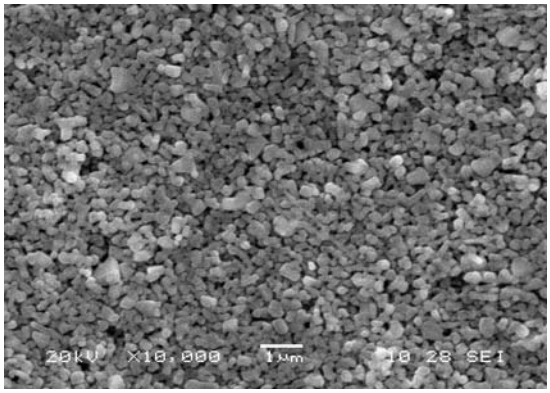

Fig.2a.SEM of Pure ZnO film

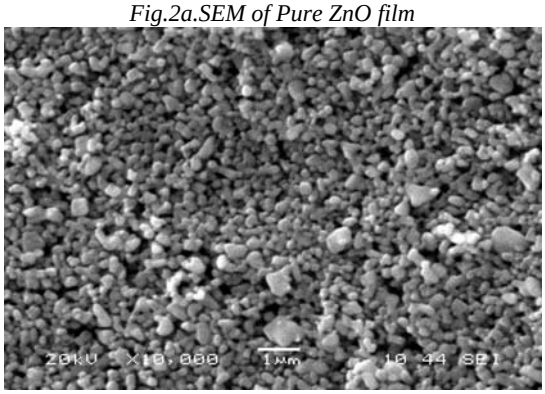

Fig.2b.SEM of 1 wt. % Al: ZnO film

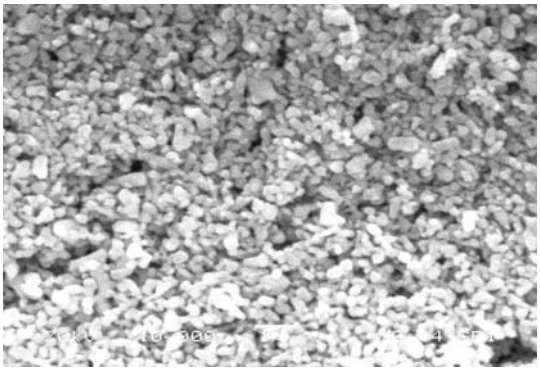

Fig.2c.SEM of 3 wt. % Al: ZnO film

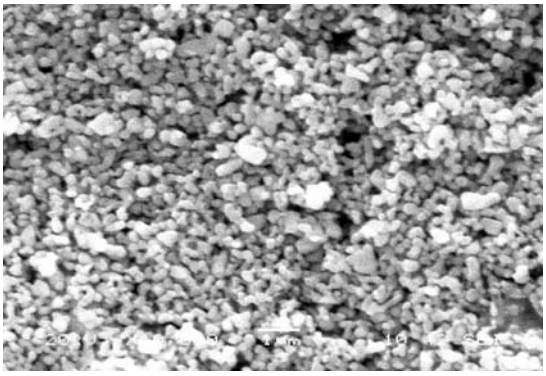

Fig.2d.SEM of 5 wt. % Al: ZnO film

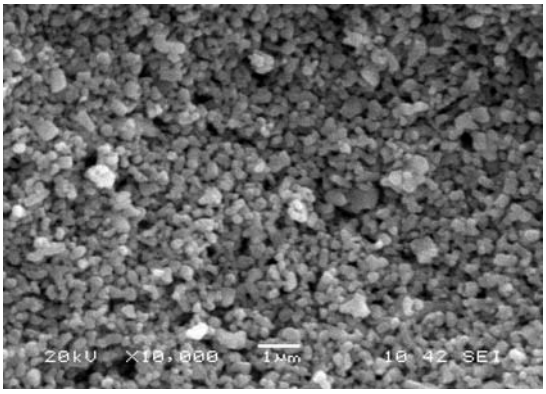

Fig.2e.SEM of 7 wt.% Al: ZnO film

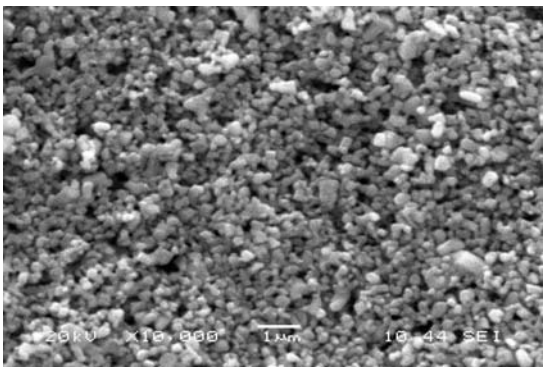

Fig.2f.SEM of 10 wt.%Al: ZnO film

Table 2. Particle size and surface area of ZnO- Al composite thick films.

wt. % of Al	Particle size in nm	Specific Surface Area in m^2/g
Pure ZnO	381	2.75
1	383	2.77
3	385	2.79
5	301	3.61
7	263	4.17
10	233	4.79

3.4. Gas – sensing characteristics

Fig. 3 shows the gas sensitivity of pure ZnO and different wt. % Al doped ZnO thick films fired at 700^{o}C exposed to 1000 ppm of CO_2 with operating temperatures. Sensitivity is the device characteristic of perceiving a variation in physical and/or chemical properties of the sensing material under gas exposure. The sensitivity of the films was determined using equation 3. The sensitivity of pure ZnO thick film to CO_2 was found to be 12.1% at 300^{0}C. Pure ZnO is notably less sensitive than doped ZnO.The sensitivity of 10 wt. % Al doped ZnO film was observed as 87.3% at 250^{0}C which is higher than other dopant concentrations. The selectivity of the films was determined using equation 4. Fig. 4-(a) shows histograms indicating the selectivity of 10wt. % of Al doped ZnO thick films for different gases against CO_2. Selectivity or specificity is defined as the ability of a sensor respond to a certain (target) gas in the presence of other gases.

Fig. 4-(b) shows variation of sensitivity of 10wt. % Al doped ZnO thick films for different gases with operating temperatures. The films showed highest selectivity to CO_2 at 250^{0}C against other tested gases viz: NH_3, LPG. H_2S, Ethanol, NO_2. Figure 5 shows the variation of sensitivity of the 10% Al doped ZnO films with CO_2concentrations (in ppm) at 250^{o}C temperature. The response and recovery times of 10wt. % Al doped ZnO thick films are represented in Figure 6. The response was quick (~ 25 sec) to 1000 ppm of CO_2 while the recovery was slow (~ 110 sec). The response/recovery time is an important parameter, used for characterizing sensors. It is defined as the time required to reach 90% of the final change in voltage or resistance, when the gas is turned on or off, respectively. The sensor performance obtained in this work is comparatively better than O.Lupan *et al* [23] where they could obtain 22.5 % sensitivity at 650^{o}C.

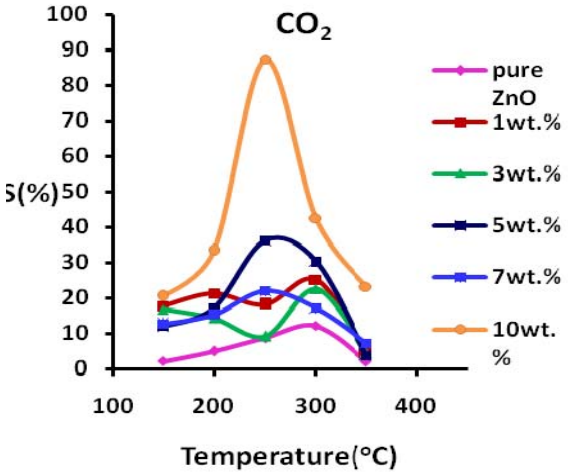

Fig.3 Gas sensitivity of pure and doped films for 1000 ppm CO_2

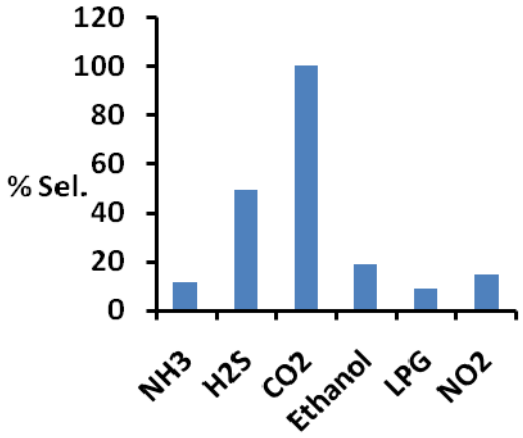

Fig.4(a) Selectivity of 10wt. % of Al: ZnO film for different gases against CO_2

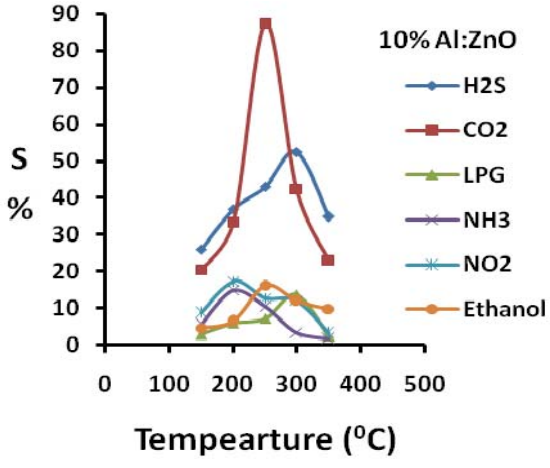

Fig.4(b) Variation of sensitivity of 10wt. % Al doped ZnO thick film for different gases with temp.

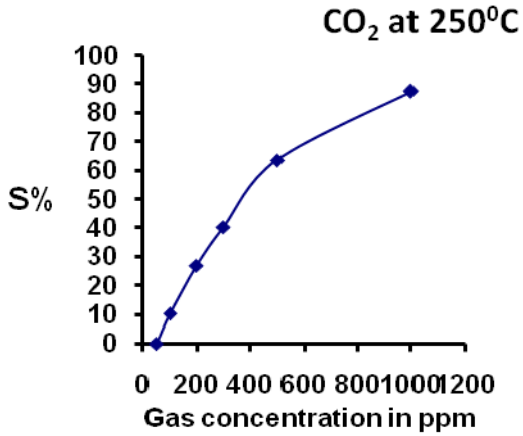

Fig.5. Variation of gas Sensitivity with gas Concentration

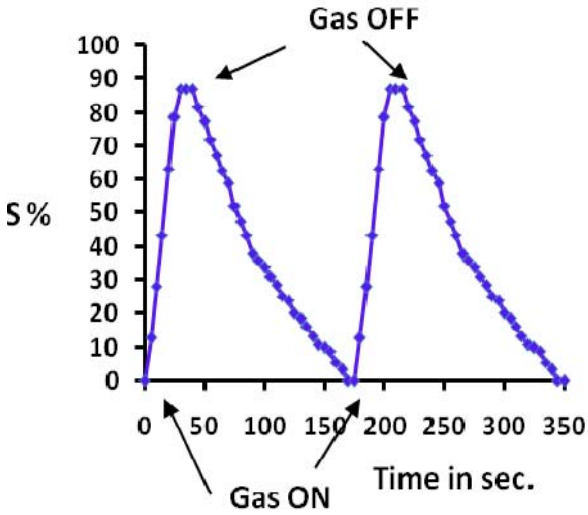

Fig.6 Response and recovery time of 10% Al doped ZnO film.

The higher response may be attributed to the optimum porosity and largest effective surface area available to react with the gas. The response could be attributed to the adsorption–desorption type of sensing mechanism. The adsorption–desorption sensing mechanism is proposed on the base of reversible chemisorptions of the carbon dioxide on the ZnO surface. It produces a reversible variation in the resistivity with the exchange of charges between carbon dioxide and the ZnO surface leading to changes in the depletion length [23, 34]. Thus, one way to improve sensitivity is to increase the change in the surface/volume ratio by adding Al like dopants [23, 35]. It is well known that oxygen is adsorbed on a ZnO surface as O^- or O^{2-} by capturing electrons [23, 36].

When Al-doped zinc oxide gas sensor is exposed to gas, the reversible chemisorptions can take place:

$$CO_2 + V^{\cdot\cdot}_o + 2e' \leftrightarrow CO + O_o^x \quad (5)$$

where $V^{\cdot\cdot}_o$ is a double positive charged oxygen vacancies, e' is negatively charged electron, O_o^x is neutral oxygen in oxygen site according to the Kroger–Vink notation [37].

It is obvious from the figure 4(b) that operating temperature plays a vital role in determining the response of the film. In fact, there exists an optimum operating temperature of a sensor to achieve the maximum response to a gas of interest, the temperature being dependent upon the kind of gases, i.e. the mechanism of dissociation and further chemisorptions of a gas on the particular sensor surface [38]. Also, the adsorption of atmospheric oxygen on the film surface depends upon the operating temperature.

The temperature (thermal energy) at which the gas response is maximum is the actual thermal energy required to activate the material for progress in reaction. However the response decreases at higher operating temperature, as the oxygen adsorbates are desorbed from the surface of the sensor [39]. Also at higher temperature, the carrier concentration increases due to intrinsic thermal excitation and Debye length decreases. This may be one of the reasons for decreased gas response at higher temperature [40].

At a low operating temperature, the response of the films to CO_2 is restricted by the speed of the chemical reaction because the gas molecules do not have enough thermal energy to react with the surface adsorbed oxygen species. In fact, during adsorption of atmospheric oxygen on the film surface, a potential barrier to charge transport is developed.

When the optimum amount of Al (10 wt. %) is incorporated on the surface of the ZnO film, Al or Al_2O_3 species would be distributed uniformly throughout the surface of the film. As a result the initial resistance of the film is high and this amount would also be sufficient to promote the catalytic reaction effectively and the overall change in the resistance on the exposure of CO_2 gas leading to an increase in the sensitivity. When the amount of Al or Al_2O_3 on the surface of the film is less than the optimum, the surface dispersion may be poor and the sensitivity of the film is observed to be decreased since the amount may not be sufficient to promote the reaction more effectively.

The 10 wt. % Al: ZnO films were exposed to different concentrations of CO_2. The sensitivity values were observed to have increased by increasing the gas concentration up to 1000 ppm. The response was highest for 1000 ppm of CO_2. From the above graph, it has been observed that the sensitivity of thick films for CO_2 at 250^oC increases linearly with increase in gas concentration upto 500 ppm. Above 500 ppm the increase in sensitivity is slow and almost saturates at 1000 ppm.Thus the active region of the sensor would be up to 500 ppm. At lower gas concentrations, the unimolecular layer of gas molecules would be formed on the surface of the sensor which could interact more actively giving larger response. At the higher gas concentrations, the multilayer of gas molecules may formed that would result into saturation in response beyond 500 ppm. The excess gas molecules would remain idle and would not reach the surface active sites of the film. So, the response at higher concentrations of the gas was not expected to increase in large extent [41].

The quick response may be due to faster oxidation of gas. The aluminum species catalyses the reaction promoting the rapid electron transfers between the adsorate and substrate.

4. Conclusions

From the results obtained, following conclusions can be made for the sensing performance of Al doped ZnO thick films,

It has become possible to make thick film gas sensors using screen printing method.

Pure ZnO thick films showed low response to CO_2.

10wt. % Al doped ZnO thick films showed highest response to CO_2 at 250^0C.

The sensitivity increases in proportion to the test gas concentration upto 500ppm and then increase is slow.

The sensor has good selectivity to CO_2 against LPG, NH_3, H_2S, Ethanol and NO_2 at 250^0C.

The sensor showed very rapid response and slower recovery to CO_2.

Acknowledgments

The authors thank management authorities of M.G. Vidyamandir Malegaon camp Dist:-Nasik, The Principal, M.S.G. College, Malegaon and the Principal, L.V.H. College, Nashik for providing all the required infrastructural facilities for doing this work.

References

[1] H.Meixner, J.Gerblinger, U.Lampe, M.Fleischer, Sensors and Actuators **23**,119 (1995).
[2] T.Takeuchi, Sensors and Actuators B **14**, 109 (1988).
[3] J.T.Woestsman, E.M.Logothetis, Controlling Automotive Emissions, the Industrial Physicist 20-24, Ed.American Institute of Physics (1995)
[4] W.Gopel, G.Reinhardt, Metal oxide Sensors: New devices through tailoring interfaces on the atomic scale, Sensors and Actuators update vol.1 H.Baltes, W.Gopel, J.Hesse Eds., Weinheim (1996)
[5] A.V.Patil, C.G.Dighavkar, R.Y.Borse, Sensors & Ttransducers Journal, **101**, 96 (2009).
[6] A.V.Patil, C.G.Dighavkar, S.K.Sonawane, S.J.Patil, R.Y.Borse, Sensors & Transducers Journal, , **108**, 189 (2009).
[7] C. G. Dighavkar, A.V.Patil, R.Y. Borse, Sensors & Transducers Journal **101**, 96 (2009).
[8] C.G.Dighavkar, A.V.Patil, S.J.Patil, R.Y.Borse, Sensors & Transducers Journal **109**,117 (2009).

[9] C. G. Dighavkar, A.V.Patil, S. J. Patil, R.Y. Borse, Sensors & Transducers Journal **109**, 117 (2009).
[10] V.M.Jimenez, J.P.Espinos, A.R.Gonzalez-Elipe, Sensors and Actuators B **61**, 23 (1999).
[11] Y.Shimizu, T.Maekawa, Y.Nakamura and E.Egashira,Sensors and Actuators B**46**,163 (1998).
[12] N.Yamazoe, Y.Kurokawa, T.Seiyama, Sensors and Actuators B **4**, 283 (1983).
[13] V.A.Chaudhary, I.S.Mulla and K.Vijayamohanan, Sensors and Actuators B **55**,154 (1999).
[14] T.Steiner, Semiconductor Nanostructures for Optoelectronic Applications, Artech House, Inc. 2004.
[15] D.C.Look, J.W. Hemsky, J.R. Sizelove, Phys. Rev. Lett., **82**, 2552 (1999).
[16] M. Suchea, S. Christoulakis, N. Katsarakis, T. Kitsopoulos, G. Kiriakidis, Thin Solid Films, **515**, 6562 (2007).
[17] A. E. Jimenez-Gonzalez, Journal of Solid-State Chemistry **28**, 176 (1997).
[18] Y. Cao, L. Miao, S. Tanemura, M. Tanemura, Y. Kuno, Y. Hayashi, Y.Mori, J. J. Appl. Phys. **45** 1623 (2006).
[19] S. H. Jeong, B. N. Park, D. G. Yoo, J. H. Boo, Journal of the Korean Physical Society **50** 622 (2007).
[20] J. Nishino, S. Ohshio, K. Kamata, J. Am. Ceram. Soc. **75**, 3469 (1992).
[21] S. Mondal, K. P. Kanta and P. Mitra, Journal of Physical Sciences **12**, 221 (2008).
[22] Chanipat Euvananont, Supattra Pakdeesathaporn, Pawilas Pratoomwan, Visittapong Yodsri, Yot Boontongkong, Chanchana Thanachayanont, and Chris Boothroyd, Journal of Microscopy Society of Thailand **22**, 26 (2008).
[23] O. Lupan, L. Chow, S. Shishiyanu, E. Monaico, T. Shishiyanu, V. S.Ontea, B. Roldan Cuenya, A. Naitabdi, S. Park, A. Schulte, Materials Research Bulletin, **44**, 63 (2009).
[24] Shih Min Chou, Lay Gaik Teoh, Wei Hao Lai, Yen Hsun Su and Min Hsiung Hon, Sensors, **6**, 1420 (2006).
[25] P.P. Sahay, R.K. Nath, Sensors and Actuators B **133**, 222 (2008).
[26] http://en.wikipedia.org/wiki/Carbon_dioxide
[27] ISBT Carbon Dioxide Quality Guidelines and Analytical Procedure Bibliography, International Society of Beverage Technologists, USA, March 2001.
[28] B.D.Cullity, Elements of X-ray diffraction 2nd Edition, Addison Wesley, 1978
[29] Gao, L., Li, Q., Song, Z., Wang, Sensors and Actuators B **71**,179 (2000).
[30] D.R.Patil, L.A.Patil, D.P.Amalnerkar, Bull.Mater. Sci., **30**, 553 (2007).
[31] B. Ismail, M. Abaab_, B. Rezig, Thin Solid Films **383**, 92 (2001).
[32] L.Y. Kupriyanov, Semiconductor Sensors in Physico-Chemical Studies, Elsevier, Amsterdam 1996
[33] Seong Hun Jeong, Bit Na Park, Dong-Geun Yoo and Jin-Hyo Boo, Journal of the Korean Physical Society **50**, 622 (2007).
[34] H.L. Hartnagel, A.L. Dawar, A.K. Jain, C. Jagadish, Semiconducting Transparent Thin Films, IOP, Bristol, 1995.
[35] J. Riu, A. Maroto, F.X. Rius, Talanta 69, 288 (2006).
[36] A.R. Raju, C.N.R. Rao, Sensors and Actuators B, **3**, 305 (1991).
[37] F.A. Kroger, in: R.N. Schock (Ed.), Point Defects in Minerals, American Geophysical Union, Washington, 1985, 1–17.
[38] P.P. Sahay, J. Mater. Sci. **40**, 4383 (2005).
[39] H.Windischmann, P.Mark, J. Electrochem. Soc. **126**, 627 (1979).
[40] J.Mizsei, Sensors and Actuators B **23**, 173 (1995).
[41] J. Arbiol, J. Cerda, G. Dezanneau, A. Cirera, F. Peiro, A. Cornet, J. R. Morante, Journal of Applied Physics **92**, 853 (2002).

*Corresponding author: aruptl@gmail.com